Toxicology Reports 7 (2020) 805–815

Contents lists available at ScienceDirect

Toxicology Reports

journal homepage: www.elsevier.com/locate/toxrep

# Early microRNA indicators of PPARα pathway activation in the liver

Brian N. Chorley[a,*], Gleta K. Carswell[a], Gail Nelson[a], Virunya S. Bhat[b,1], Charles E. Wood[a,2]

[a] Office of Research and Development, U.S. EPA, Research Triangle Park, North Carolina, 27711, USA
[b] NSF International, Ann Arbor, Michigan, 48105, USA

ARTICLE INFO

*Keywords:*
MicroRNAs
Biomarkers
Mode of action (MOA)
Adverse outcome pathway (AOP)
Benchmark dose (BMD)
Peroxisome proliferator-activated receptor alpha (PPARα)
Liver toxicity
Hepatocellular carcinoma
Phthalate

ABSTRACT

MicroRNAs (miRNAs) are short non-coding RNA species that play key roles in post-transcriptional regulation of gene expression. MiRNAs also serve as a promising source of early biomarkers for different environmental exposures and health effects, although there is limited information linking miRNA changes to specific target pathways. In this study, we measured liver miRNAs in male B6C3F1 mice exposed to a known chemical activator of the peroxisome proliferator-activated receptor alpha (PPARα) pathway, di(2-ethylhexyl) phthalate (DEHP), for 7 and 28 days at concentrations of 0, 750, 1500, 3000, or 6000 ppm in feed. At the highest dose tested, DEHP altered 61 miRNAs after 7 days and 171 miRNAs after 28 days of exposure, with 48 overlapping miRNAs between timepoints. Analysis of these 48 common miRNAs indicated enrichment in PPARα–related targets and other pathways related to liver injury and cancer. Four of the 10 miRNAs exhibiting a clear dose trend were linked to the PPARα pathway: mmu-miRs-125a-5p, -182−5p, -20a−5p, and -378a−3p. mmu-miRs-182−5p and -378a−3p were subsequently measured using digital drop PCR across a dose range for DEHP and two related phthalates with weaker PPARα activity, di-*n*-octyl phthalate and n-butyl benzyl phthalate, following 7-day exposures. Analysis of mmu-miRs-182−5p and -378a−3p by transcriptional benchmark dose analysis correctly identified DEHP as having the greatest potency. However, benchmark dose estimates for DEHP based on these miRNAs (average 163; range 126−202 mg/kg-day) were higher on average than values for PPARα target genes (average 74; range 29−183 mg/kg-day). These findings identify putative miRNA biomarkers of PPARα pathway activity and suggest that early miRNA changes may be used to stratify chemical potency.

## 1. Introduction

In 2007, the National Research Council released guidance on next generation toxicity testing that called for increased use of short-term biomarkers [1,2]. A key requirement of this new paradigm is the linkage between early molecular-based measurements and their associated adverse health effects. This general concept has served as the basis for the mode-of-action (MOA) and, more recently, the adverse outcome pathway (AOP), which distill complex biological processes into sequential key events or key event networks leading to an adverse health outcome [3,4]. These constructs currently serve an important role in the organization and review of mechanistic data and the identification of key data gaps. This type of pathway-based information also supports tiered testing strategies for chemical risk determination as required under the Frank R. Lautenberg Chemical Safety for the 21 st Century Act, a 2016 reform of the U.S. Toxic Substances Control Act (TSCA). Moving forward, however, predictive applications will require more targeted pathway-specific biomarkers and a greater

*Abbreviations:* *Acox1*, acyl-Coenzyme A oxidase 1; AOP, adverse outcome pathway; AIC, Akaike Information Criterion; ALT, alanine aminotransferase; $BMD_A$, apical-based benchmark dose; AhR, aryl hydrocarbon receptor; AST, aspartate aminotransferase; BMD, benchmark dose; BMR, benchmark response; BROD, benzyloxyresorufin O-debenzylation; BMDL, BMD lower confidence interval; CAR, constitutive androstane receptor; DEHP, di (2-thylhexyl) phthalate; DEGs, differentially expressed genes; DEmiRs, differentially expressed miRNAs; DNOP, di-*n*-octyl phthalate; ddPCR, droplet digital polymerase chain reaction; EROD, ethoxyresorufin O-dealkylation; GEO, Gene Expression Omnibus; HCA, hepatocellular adenoma; HCC, hepatocellular carcinoma; IPA, Ingenuity Pathway Analysis; mRNA, messenger RNA; miRNAs, microRNAs; mtDNA, mitochondrial; MOA, mode of action; BBP, *n*-butyl benzyl phthalate; Nrf2, nuclear receptor erythroid 2-like 2; PROD, pentoxyresorufin O-depentylation; PPARα, peroxisome proliferator-activated receptor alpha; POD, point-of-departure; PXR, pregnane X receptor; rRNA, ribosomal RNA; smallRNA-seq, small RNA sequencing; SDH, sorbitol dehydrogenase; $BMD_T$, transcriptional-based benchmark dose; tRNA, transfer RNA; TMM, trimmed mean of M-values; EPA, U.S. Environmental Protection Agency

* Corresponding author at: MD-B105-03, 109 T.W. Alexander Drive, U.S. Environmental Protection Agency, Research Triangle Park, NC, 27709, USA.
*E-mail address:* chorley.brian@epa.gov (B.N. Chorley).
[1] Current address: ToxStrategies, Boston, MA 01749.
[2] Current address: Boehringer Ingelheim Pharmaceuticals, Inc., Ridgefield CT 06877.

https://doi.org/10.1016/j.toxrep.2020.06.006
Received 4 March 2020; Received in revised form 1 June 2020; Accepted 19 June 2020
Available online 23 June 2020

understanding of quantitative relationships between early and late key events (Meek et al., 2014; Simon et al., 2014).

Recent work has highlighted the potential value of short-term transcriptomic-based measurements to identify surrogate points-of-departure (PODs) for chemical screening [5–11]. A common challenge in these studies is selecting appropriate gene targets linked to specific pathways and associated adverse effects [12]. There are a numerous examples that have used transcriptomic biomarkers to determine cellular perturbations or outcomes, including activation or suppression of nuclear receptors, genotoxicity, cellular stress and proliferation, and a wide variety of other biological and toxicological effects [13–16]. Another example is the S1500+ gene compendium, which was constructed to include "sentinel" genes altered by chemical exposure that are representative of common toxicological responses in many cell types without having to measure the full transcriptome [17]. However, currently there are few standardized gene targets for specific MOAs/AOPs and limited information linking quantitative changes in gene expression to later health outcomes [6,8].

MicroRNAs (miRNAs) are short non-coding RNA molecules, usually 22–24 nucleotides in length, that regulate gene expression post-transcriptionally by binding complementary sequences on messenger RNA (mRNA) and inducing degradation of the mRNA or suppression of gene translation [18–20]. In contrast to the tens of thousands of transcribed mRNAs in mammals, the known complement of expressed mature miRNAs is about a magnitude less, with approximately 2700, 2000, and 800 known in human, mice, and rats, respectively (miRBase build 22; http://www.mirbase.org). Computational and experimental analyses estimate that a single miRNA may have hundreds of gene targets, and that miRNAs overall may impact approximately 30–80 % of transcribed genes, depending on cell and tissue [19,21,22]. A small number of miRNAs can thus impact a large number of genes, with less global cell-to-cell variability compared to mRNAs [23,24]. In cancer profiling studies, a select number of miRNAs can provide robust prediction of tumor lineage and differentiation [25]. In addition, miRNAs can serve an indicators of acute environmental chemical exposures [26], including activation of nuclear receptors and other transcription factors [26–28], exhibit dose-responsiveness [9], and appear in measurable quantities within accessible biofluids [29], which may enable biosurveillance efforts. Given these characteristics, miRNAs are being widely investigated as biomarkers of both chemical exposure and susceptibility to later adverse health outcomes.

In this case study, we evaluated alterations of liver miRNAs following short-term exposure to chemicals with documented peroxisome proliferator-activated receptor alpha (PPARα) activity in the liver [8,30–32]. This pathway is a common target of environmental chemicals that mediates a diverse array of metabolic and carcinogenic effects in animal models [30]. For example, it has been demonstrated that PPARα activation may mediate developmental and immunotoxicity in rodents induced by the persistent organic pollutants perfluorooctane sulfonate (PFOS) and perfluorooctanoic acid (PFOA) and modulate downstream pathways involved in metabolism, cell growth and differentiation, and inflammation [33,34].

Our current work builds on previous studies showing that early measures linked to PPARα activity, including transcriptional-based benchmark dose ($BMD_T$) estimates for known PPARα target genes, can be used to estimate dose potencies and stratify chemicals based on later-life effects [8]. Male B6C3F1 mice were exposed for 7 and 28 days to three reference phthalates, di (2-ethylhexyl) phthalate (DEHP), di-*n*-octyl phthalate (DNOP), and *n*-butyl benzyl phthalate (BBP). These chemicals vary widely in PPARα activity, as indicated by our previous data [8,32]. Effects included dose-responsive hepatocellular cytoplasmic alteration typical of peroxisome proliferation [35], increased cyanide-insensitive palmitoyl CoA oxidase (PCO) activity, which is dependent on the PPARα-dependent gene *Acox1* [36], and marked gene expression responses consistent with PPARα activation. PPARα-mediated effects of DEHP were further corroborated in PPARα-null mice, which demonstrated that approximately 94 % of the induced transcriptional activity in wild-type mouse liver were dependent on PPARα [37,38]. In the current study, we used small RNA sequencing (small RNA-seq) to assess global alterations in mouse liver miRNAs due to phthalate exposure and link these changes with known biological pathways. We estimated BMDs based on sequencing and digital-drop PCR (ddPCR) measurements, compared these values to referent $BMD_T$ and apical ($BMD_A$) estimates, and assessed concordance between liver and serum miRNA targets. While our findings identify miRNAs that may serve as early biomarkers of PPARα pathway activity, transcriptional responses were closer to BMD estimates for adverse apical outcomes.

## 2. Materials and methods

### 2.1. Chemicals

Phthalates were purchased from Chem Service (West Chester, PA). DEHP (99.5 % purity, lot number 253900), BBP (99 % purity, lot number 853100), and DNOP (99.5 % purity, lot number 834400) were added to AIN93 G rodent diet (TestDiet, Richmond, IN) by the vendor. Control AIN93 G diet was processed in the same way as diets with phthalate added.

### 2.2. Study design

The experimental design and treatment protocols have been described previously [8]. Briefly, weanling male B6C3F1 mice were obtained at approximately 21 days from Charles River Laboratories (Raleigh, NC) and cared for under protocols approved by the Institutional Animal Care and Use Committee of the U.S. Environmental Protection Agency (EPA). Body weight and food and water consumption were monitored throughout this period to ensure similar treatment group starting conditions.

When the mice reached a minimum of 65 days of age, they were dosed for 7 days with either control diet or diet containing DEHP (750, 1500, 3000, and 6000 ppm), DNOP (1250, 2500, 5000, and 10,000 ppm), or BBP (1500, 3000, 6000, and 12,000 ppm). Some mice were also fed 6000 ppm DEHP for 28 days to examine persistent effects. On the day of sacrifice (either 7 or 28 days after the start of treatment), body and liver weights were recorded, and liver tissue including left lateral, caudate, and right medial liver lobes was immediately flash frozen in liquid nitrogen and stored at −80 °C until further processing. Serum samples were processed from blood obtained via cardiac puncture and stored at −80 °C.

### 2.3. RNA isolation from tissue

Total RNA was isolated from approximately 20 mg of frozen liver tissue homogenized in

RNAzol RT (Molecular Research Center, Cincinnati, OH) followed by purification with the RNeasy MinElute column protocol modified to retain the small RNA (Qiagen GmbH, Hilden, Germany). Initial yield was quantified by the NanoDrop spectrophotometer (NanoDrop Technologies, Wilmington, DE). RNA quality was assessed by the Agilent RNA6000 kit assay on the Agilent 2100 Bioanalyzer (Agilent Technologies, Berlin, Germany). The RNA was DNase-treated using a Turbo DNase treatment (ThermoFisher Scientific, Waltham, MA) followed by Qiagen MinElute cleanup. Total RNA was quantitated using the Qubit Broad Range RNA assay (ThermoFisher Scientific).

### 2.4. RNA isolation from serum

Total RNA was extracted from archived frozen serum (50 µL/mouse) using the miRCURY RNA Isolation Kit for Biofluids (Exiqon Inc., Woburn, MA). Isolation followed the manufacturer's instructions, with the exception that glycogen carrier (ThermoFisher Scientific) and

Exiqon RNA spike-ins were added to the lysis solution to increase small RNA yield and serve as internal controls for sample quality control, respectively.

### 2.5. miRNA library preparation and sequencing

The CleanTag Small RNA Library Prep Kit (TriLink Biotechnologies, San Diego, CA) and protocol was used to prepare the sequencing library. For the liver samples, 500 ng of total RNA was used as input. All reaction parameters were set as described in the protocol, including use of Illumina small RNA index primers in the library amplification. After amplification, the library was bead-purified according to manufacturer's instructions. Purified library quality was assessed using the High Sensitivity DNA kit on the Agilent 2100 Bioanalyzer, and concentration was determined by the Qubit dsDNA High Sensitivity Assay (ThermoFisher Scientific).

Sequencing was performed on the NextSeq 500 using the NextSeq Mid Output kit (Illumina Inc., San Diego, CA). Quantitation of the purified libraries was based on the peaks identified on the HS DNA Bioanalyzer chip analysis as per TriLink Biotechnologies recommendation. Sequencing run parameters were as specified by Illumina using a single-end read at 50 cycles. Sequencing data have been deposited to the National Center for Biotechnology Information Gene Expression Omnibus (GEO) (https://www.ncbi.nlm.nih.gov/geo/) under accession number GSE144988.

### 2.6. Sequencing analysis

The generated reads were checked for quality and trimmed of adapter sequence using the Illumina BaseSpace Application. The processed FastQ files were analyzed using the Partek Flow (version 6.0) software program (Partek, St. Louis, MO). Sequences were further trimmed from both 5' and 3' ends if the Phred quality score was less than 20. Samples were aligned with Bowtie version 1.0.0 to the mm10 reference index using up to a 1 base pair mismatch and seed length of 10. Aligned sequences were then annotated to miRBase mature miRNA version 21 with the Partek E/M (expectation maximum) algorithm. MiRNA counts were normalized with TMM (trimmed mean of M-values) and a 0.0001 count was added to all features. Negative binomial regression was used to model the normalized count data when determining differentially expressed miRNAs (DEmiRs). Significance testing was corrected for multiple tests and was determined by a Storey q-value of $p \leq 0.05$. Samples were dropped from analysis if there were less than one million total reads or less than 10 % of the counts were fully or partially aligned within miRNA features. Features (miRNAs) were excluded if the geometric mean across all samples was less than or equal to 10.

### 2.7. ddPCR

Profiling of selected miRNAs by polymerase chain reaction (PCR) was performed using the Universal cDNA synthesis kit and microRNA LNA PCR primer sets (Exiqon Inc.) with the QX200 Droplet Digital PCR (ddPCR) System and EvaGreen Supermix (Bio-Rad Laboratories, Hercules, CA). Due to low concentration, RNA concentrations in serum extractions cannot be determined accurately; therefore, equal starting volumes of serum RNA were used as input. For liver, 10 ng of total RNA was input per reverse transcriptase reaction. cDNA dilution factors were determined empirically for each sample type and miRNA target. The ddPCR experimental workflow consisting of droplet generation, PCR amplification, droplet reading, and data analysis was performed according to the manufacturer's instructions. The droplet reader and QuantaSoft™ software were used in absolute quantification mode to count PCR-positive and PCR-negative droplets and determine the starting concentration of the target DNA molecule. The threshold separating positive and negative droplets was manually set at just below the positive cluster on a well-by-well basis.

### 2.8. Dose-response modeling

Benchmark dose analysis was used to estimate the threshold dose at which specific genes and apical effects were altered above (or below) controls. BMD modeling of apical and transcriptional endpoints ($BMD_A$ and $BMD_T$, respectively) was performed in previous studies [8,39], and estimates were used as reference values for this study. For BMD values calculated for sequencing and ddPCR miRNA data ($BMD_{miR}$), the EPA BMDS software version 2.6.0.1 was used (https://www.epa.gov/bmds). Count data used in modeling were filtered and normalized, as described in *Sequencing Analysis*. Doses (mg/kg-day) were previously calculated from representative intake values [8]. Parameters for model calculations included a confidence level of 95 % to calculate BMD lower confidence interval ($BMD_L$) [40], benchmark response (BMR) to 1.349 to correspond to the amount of change required to shift the mean response by 10 % above background [41], and constant variance was assumed (Rho = 0), consistent with previous $BMD_A$ and $BMD_T$ modeling methods [8,39].

Five continuous model types were used to fit the data: Hill, polynomial (2° and 3°), linear, and power. The best-fit model was selected using the following criteria: 1) Polynomial and linear models were compared for best fit by comparing a nested likelihood ratio test denoted as Test #4 or "goodness-of-fit" value that exhibited a value > 0.1 within BMDS. If both polynomial and linear models exhibited a *p*-value > 0.1, then the simpler model was selected (e.g., linear). 2) The selected linear/polynomial model was then compared to the Hill and Power models and the choice of the overall best-fit model was based collectively on the weight-of-evidence considering, in preferential order, a) the lowest Akaike Information Criterion (AIC) value, b) lower local Chi scaled residuals ($\leq |2.0|$), particularly in the range of the BMD/BMDL, c) a qualitatively better visual inspection of fit, and d) the global good-of-fit p value, with p = 1 indicating a "perfect fit" (i.e., the predicted values are equal to the observed values). Models with p < 0.1 were excluded from consideration. 3) Finally, any calculated BMD values that were above the highest tested dose based on the best-fit model were discarded and noted as such in the results. In both sequencing and ddPCR data, BMD values were evaluated with and without the top doses included, an acceptable approach when there is a plateau at the highest dose to improve model fitting [40].

### 2.9. Statistics

Upward or downward trends of miRNA expression due to dose were initially conducted using a Jonckheere–Terpstra test with significant trends noted as *p*-values < 0.05. Expression results from ddPCR measurements were reported as a concentration (copies of miRNA per µl of assay volume). Boxplots of the data, which were generated using BoxPlotR (http://shiny.chemgrid.org/boxplotr/), display the maximum value (upper whisker), third quartile (upper box), median (midline), first quartile (lower box), minimum (lower whisker), and mean (cross) data values. Individual sample data are plotted as open circles, with outliers displayed outside the minimum and maximum value whiskers. Most groups did not display a normal distribution of data according to a Shapiro-Wilk Normality Test (*p*-value < 0.05); therefore, a Mann-Whitney *U* test was conducted to determine significant differences of treatment group miRNA expression from control groups (*p*-value < 0.05). Clustering analysis was performed by using an average linkage cluster distance metric and Euclidean point distance metric. Feature signals on heatmaps were standardized by shifting the feature mean to 0 and scaling the standard deviation to 1 to normalize visualization. Molecular and cellular function, toxicity, disease, upstream regulator, and target mRNA predictions were performed in Ingenuity Pathway Analysis software (IPA) (Qiagen). Pathways were considered enriched based on a Fisher's exact score of *p*-value < 0.05 with false discovery

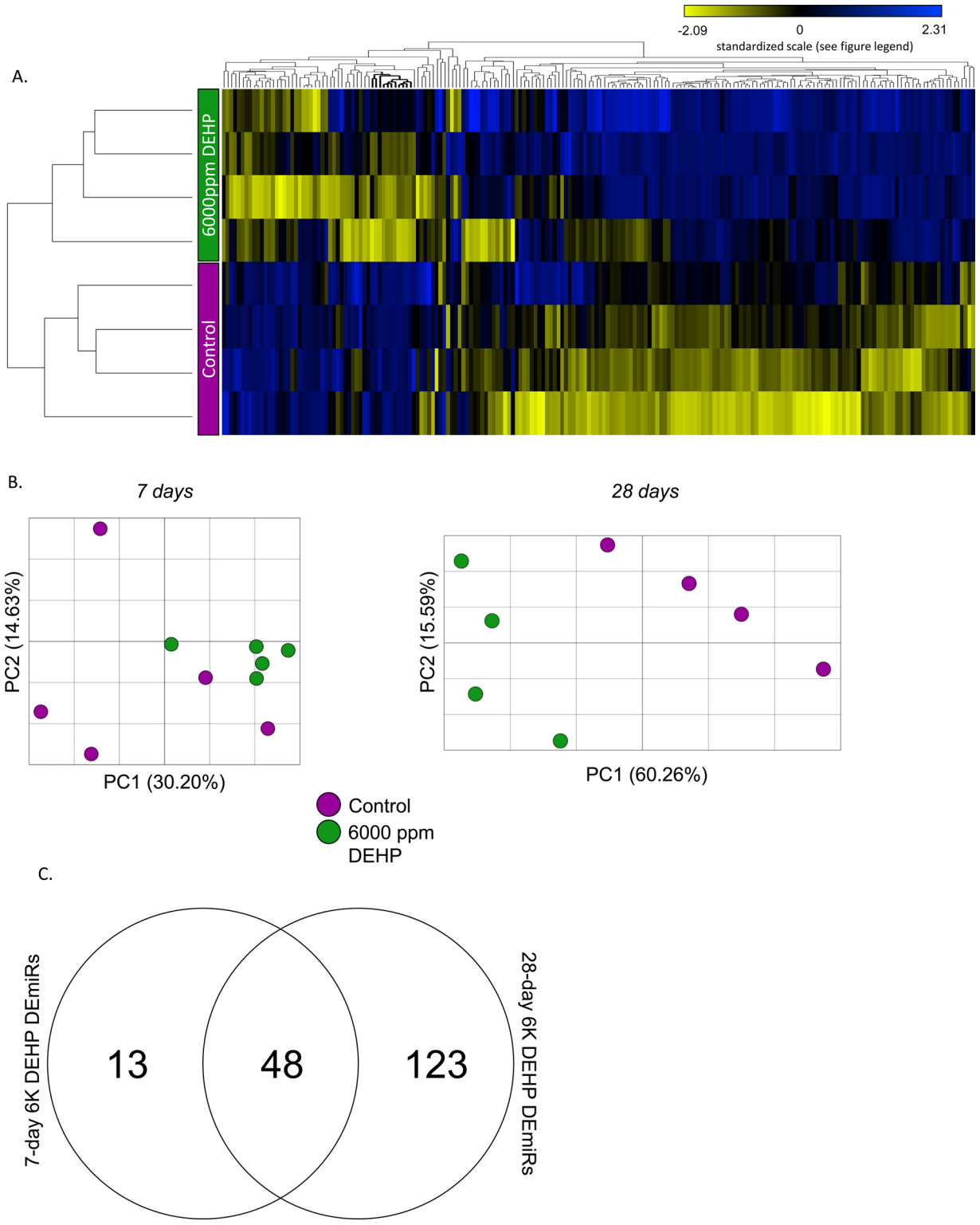


**Fig. 1. Global analysis of mouse liver miRNA alterations after short-term DEHP exposure.** Male B6C3F1 mice were exposed to DEHP for 7 or 28 days through diet and liver miRNA alterations were measured using small RNA-seq. Significant differences were observed at both timepoints, with more robust miRNA alterations occurring at the later timepoint. (**A**) Average linkage clustering using normalized miRNA counts indicated clear distinct groupings of high (6000 ppm) treated and control mice after 28 days of exposure. (**B**) Principal component analysis (PCA) similarly indicated these differences at 28 days, but the groups were less distinct at the earlier time with the highest dose tested. (**C**) Forty-eight differentially expressed miRNAs (DEmiRs) were in common after 7 and 28 days of high DEHP exposure.

rate correction for multiple tests.

## 3. Results

### 3.1. Global microRNA expression analysis

Small RNA-seq was used to measure altered miRNAs in liver tissue from male mice exposed to DEHP for 7 days (750, 1500, 3000, and 6000 ppm) and 28 days (6000 ppm only). The 6000 ppm dose of DEHP altered miRNA expression compared to the control group after 28 days of exposure, based on hierarchal clustering of differentially expressed miRNAs (DEmiRs) (Fig. 1A) and principal component analysis (PCA) (Fig. 1B). A total of 171 DEmiRs were significantly altered at this later time point. Differences in DEmiR profiles were not as apparent on PCA among DEHP dose groups after 7 days of exposure (Supplemental Fig. 1), similar to previous analysis of differentially expressed mRNAs in this study [8]. Consequently, fewer DEmiRs (61) were noted between the highest dose group and the control group (Fig. 1B). Of these, 48 overlapped with those observed after 28 days of exposure at the same dose (with 41 altered in the same direction), indicating concordance in miRNA responses over time (Fig. 1C; Supplemental File 1). Of note, mmu-let-7c-5p, previously highlighted as an inhibited miRNA by acute and long-term PPARα activation in mouse liver, was similarly inhibited by DEHP at both 7 and 28 d in our study [27].

To examine the relationship between miRNA alterations and functional or disease correlates, the 48 DEmiRs observed at both 7 and 28 days were evaluated in IPA. A core analysis was performed, which included examination of signaling pathways and processes linked to diseases and abnormalities, molecular and cellular functions, and development (Supplemental File 2, Table 1). Molecular and cellular functions that were significantly linked to these miRNAs indicated roles in cell development, growth, proliferation, and movement (Supplemental File 2, Table 1 orange highlights). In addition, disease pathway enrichment included cancer, gastrointestinal disease, organismal injury/abnormalities, and inflammation (Supplemental File 2, Table 1 blue highlights and tab 2 summary). Liver-related outcomes were frequently enriched in a separate "tox functions" analysis, including pathways related to liver cancer, hepatitis B, and fatty liver disease (Supplemental File 2, tab 3).

To predict gene targets of the DEmiRs and their involvement in toxicity pathways, we applied RNA-seq data previously generated from these same liver samples [39] (GEO Accession #GSE78962). Using a combination of target prediction algorithms (TargetScan, TarBase, and others) and experimental data within IPA, the 48 common DEmiRs were bioinformatically linked to gene expression changes after 7 days of treatment with 6000 ppm DEHP (Supplemental File 3). "Tox functions" analysis was then repeated on these 668 unique miRNA-linked differentially expressed genes (DEGs) (Supplemental File 4, Table 1). Similar to the miRNA-only analysis, toxicity pathway analysis on linked DEGs indicated roles in hepatocellular carcinoma and liver hyperplasia/hyperproliferation (Fig. 2A). Importantly, IPA "upstream regulator prediction" of the DEGs implicated PPARα and acyl-coenzyme A oxidase 1 (*Acox1*), a PPARα-regulated gene that mediates fatty acid beta-oxidation, as putative drivers of the gene/miRNA expression response (Fig. 2B, left; Supplemental File 4, tab 2). Using this same analysis module in IPA, similar upstream activators were identified when all significant DEGs (1606) from the 6000 ppm DEHP group at 7 days were analyzed from Hester et al. [39] (Fig. 2B, right; Supplemental File 4, tab 3). These predictions, based on gene expression analysis, are concurrent with previous findings that PPARα mediates the primary transcriptional response in liver in response to DEHP exposure in mice [30].

### 3.2. MiRNA dose-response after 7 days of DEHP exposure

Of the 177 measured miRNAs in mice following 7 days of DEHP exposure, 19 were identified as trending upward or downward with increasing dose, based on a two-tailed Jonckheere-Terpstra test $p$-value $< 0.05$ (Supplemental Table 1). Of these 19 microRNAs, 11 were significantly altered at the 6000 ppm DEHP dose at both 7 and 28 days exposure, and 6 have been previously linked to PPARα-dependent transcriptional response in mouse liver with short-term agonist exposure [27] (Table 1). Together, 4 miRNAs that were altered at both timepoints and linked to PPARα regulation exhibited either upward (mmu-miRs-182−5p, -378a−3p, and -125a−5p) or downward (mmu-miR-125a−5p) dose trends, with mmu-miRs-182a-5p and -378a-3p

**Table 1**
Dose-responsive miRNAs that are significantly altered in mouse liver following exposure to DEHP (in ppm) at both 7- and 28-day timepoints.

DEHP *vs.* control fold change *[95% upper, lower limit]*

| | 7 days | | | | | | | | 28 days | |
|---|---|---|---|---|---|---|---|---|---|---|
| microRNA | 750 | | 1500 | | 3000 | | 6000 | | 6000 | |
| mmu-miR-125a-5p┼ | **−3.03**** | | **−3.00**** | | **−2.54*** | | **−4.46**** | | **−2.16**** | |
| | *[-5.60,* | *−1.64]* | *[-5.20,* | *−1.73]* | *[-4.56,* | *−1.42]* | *[-8.36,* | *−239]* | *[-3.28,* | *−1.42]* |
| mmu-miR-182−5p┼ | **1.79*** | | **3.23**** | | **5.85**** | | **5.25**** | | **9.06**** | |
| | *[1.01,* | *3.17]* | *[1.93,* | *5.41]* | *[3.40,* | *10.08]* | *[3.00,* | *9.31]* | *[4.80,* | *17.1]* |
| mmu-miR-194−2-3p | **−1.45** | | **−1.71** | | **−1.79*** | | **−1.98*** | | **1.28*** | |
| | *[-2.65,* | *1.27]* | *[-2.95,* | *1.01]* | *[-3.22,* | *1.00]* | *[-3.67,* | *−1.07]* | *[-1.26,* | *2.07]* |
| mmu-miR-20a-5p┼ | **1.64** | | **2.35** | | **2.71** | | **2.52*** | | **−1.35*** | |
| | *[-1.52,* | *4.07]* | *[1.03,* | *5.33]* | *[1.14,* | *6.47]* | *[1.01,* | *6.24]* | *[-2.42,* | *1.33]* |
| mmu-miR-320−3p | **−5.47**** | | **−4.39**** | | **−2.39** | | **−6.88**** | | **−2.35**** | |
| | *[-11.57,* | *−2.59]* | *['8.55,* | *−2.25]* | *[-4.82,* | *−1.19]* | *['14.67,* | *−3.23]* | *['-4.88,* | *−1.13]* |
| mmu-miR-339−5p | **−1.27** | | **1.55*** | | **−2.09*** | | **−1.59*** | | **1.52*** | |
| | *[-1.83,* | *1.14]* | *[-2.16,* | *−1.11]* | *[-3.02,* | *−1.45]* | *[-2.31,* | *−1.09]* | *[-1.05,* | *2.45]* |
| mmu-miR-378a-3p┼ | **1.12** | | **1.13** | | **1.58*** | | **1.42*** | | **2.35**** | |
| | *[-1.22,* | *1.53]* | *[-1.17,* | *1.5]* | *[1.17,* | *2.13]* | *[1.04,* | *1.93]* | *[1.81,* | *3.06]* |
| mmu-miR-423−5p | **−1.95*** | | **−1.41** | | **−1.65** | | **−2.32*** | | **1.26*** | |
| | *[-1.32,* | *3.6]* | *[-1.08,* | *3.77]* | *[-1.5,* | *2.95]* | *[1.01,* | *4.78]* | *[1.3,* | *2.09]* |
| mmu-miR-455−3p | **−5.3**** | | **−4.93*** | | **−3.31*** | | **−12.28*** | | **−15.98**** | |
| | *[-12.44,* | *−2.26]* | *[-10.58,* | *−2.3]* | *[-7.42,* | *−1.48]* | *[-29.62,* | *−5.09]* | *[-28.98,* | *−8.81]* |
| mmu-miR-98−5p | **1.65** | | **1.87** | | **1.4** | | **2.2*** | | **1.65**** | |
| | *[-1.32,* | *3.6]* | *[-1.08,* | *3.77]* | *[-1.5,* | *2.95]* | *[1.01,* | *4.78]* | *[1.3,* | *2.09]* |

* q-value ≤ 0.05.
** q-value ≤ 0.005; ┼PPARα dependent.

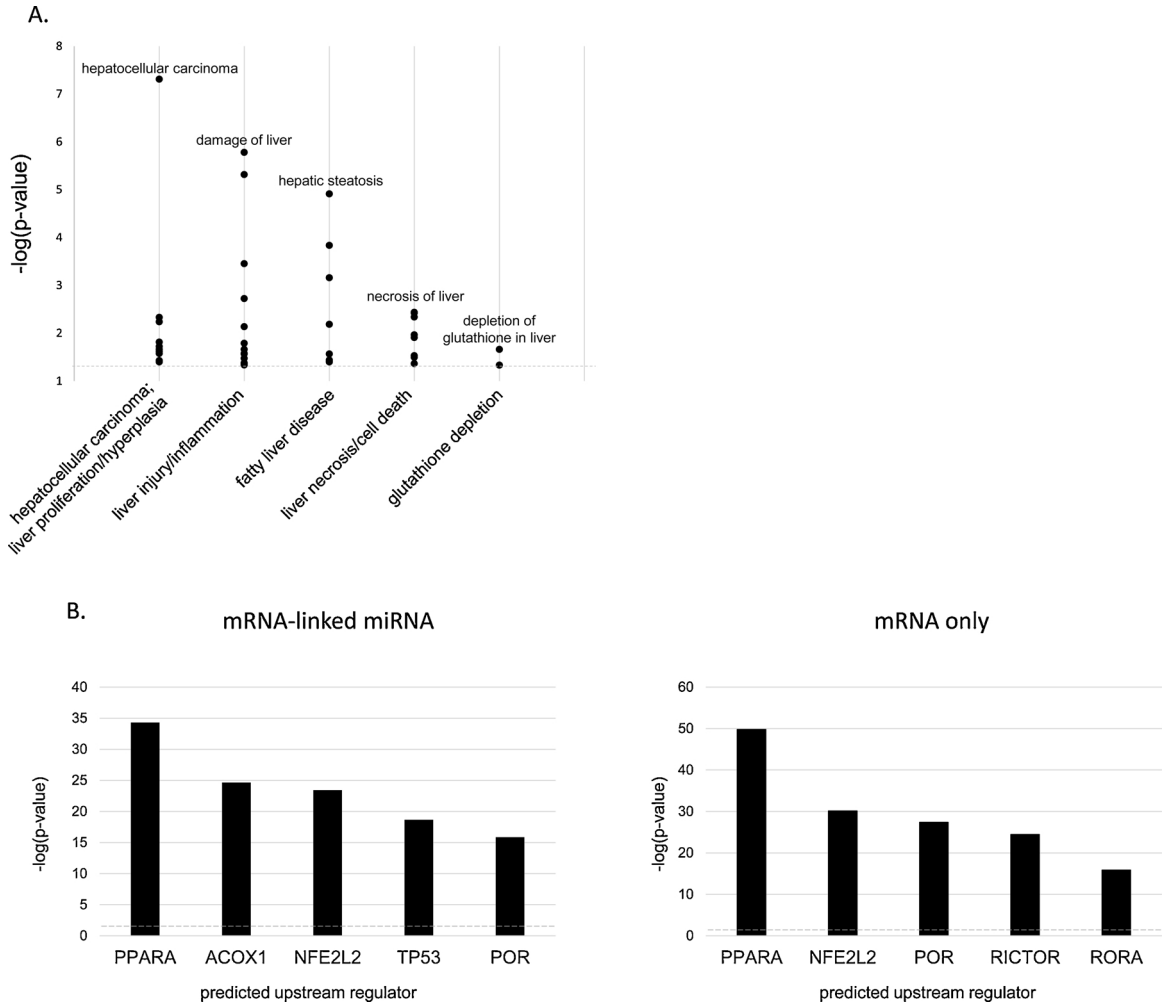


**Fig. 2. Ingenuity Pathway Analysis (IPA) of mRNA linked to altered miRNA at 7 and 28 days following 6000 ppm DEHP exposure.** Differentially expressed genes (DEGs) were linked to DEmiRs using the miRNA target prediction algorithms in IPA. These predicted miRNA target genes were analyzed for signaling pathway enrichment using IPA: (**A**) toxicological pathway lists and (**B**) upstream regulator analysis. For the toxicity analysis, each dot represents a different pathway that was significantly enriched by this DEG list (-log(*p*-value > 1.3) and related to the general category listed along the x-axis. These pathways are fully described in Supplemental File 4, under "miRNA.linked DEGSs, tox function" and "miRNA.linked DEGs, upstream.reg" tabs.

exhibiting the lowest *p*-value for all significant trends (< 0.0001 and 0.0059, respectively). These miRNAs also correlated with dose-responsive expression due to DEHP exposure in genes that were linked to the PPARα pathway [39]. The correlation between candidate miRNAs and PPARα target gene expression ($r^2$ = 0.11 – 0.67, mean = 0.41) was generally lower than that correlations amongst the PPARα target genes themselves ($r^2$ = 0.45 – 0.99, mean = 0.80). Encouragingly, miRNAs with the strongest dose trends exhibited the best correlations with PPARα-linked gene expression dose response, specifically mmu-miRs-182 – 5p (r2 = 0.46 – 0.67, mean = 0.55) and -378a-3p (r2 = 0.11 – 0.43, mean = 0.36) (Supplemental Fig. 2).

### 3.3. ddPCR validation and BMD estimates for target miRNAs

To validate sequencing values and compare responses to related chemicals with weaker PPARα activity [8], ddPCR was used to quantify candidate miRNA responses on 7-day exposure groups for DEHP, DNOP, and BBP. In addition to mmu-miR-182 – 5p and mmu-miR-378a – 3p, mmu-let-7g – 5p was measured as a putative negative control based on non-significant pairwise analysis between DEHP dose groups and controls in the sequencing results. Mmu-miR-107 – 3p was also included based on an increasing dose-trend in our data (Supplemental Table 1) and previous data including it as a PPARα-responsive miRNA [27]; therefore, we wanted to further evaluate with ddPCR as an independent measure.

Results from ddPCR confirmed many of the sequencing results from the DEHP groups (Supplemental Fig. 4). Both mmu-miRs-182 – 5p and -378a – 3p increased with dose for 750, 1500, and 3000 ppm DEHP groups, whereas values for the 6000 ppm dose was at similar or lower levels than the 3000 ppm doses. In contrast to the sequencing data, mmu-miR-107 – 3p expression was significantly increased at 3000 and 6000 ppm DEHP doses but did not exhibit a significant dose trend. BBP treatment increased mmu-miRs-182 – 5p and -107 – 3p expression at the highest dose. DNOP resulted in a dose-dependent increase in expression of mmu-miRs-378a – 3p and -107 – 3p but had no observable effect on mmu-miR-182 – 5p. As expected, mmu-let-7g-5p was not significantly altered with DEHP and BBP treatments; however, expression was significantly lower at 2500 and 5000 ppm doses of DNOP. Overall, ddPCR measurements indicated that expression of mmu-miRs-182 – 5p and -378a – 3p were most responsive to DEHP, whereas exposure to the two weaker PPARα-activating phthalates, BBP and DNOP, resulted in either no effect or effects only at the highest doses tested.

To further evaluate miRNA dose responses, and to generate values that could be compared to other endpoints previously generated for this study, BMD analyses were performed on PPARα-linked mmu-miRs-182 – 5p, -378a-3p, -20a-5p, and -107 – 3p ($BMD_{miR}$). Negative control

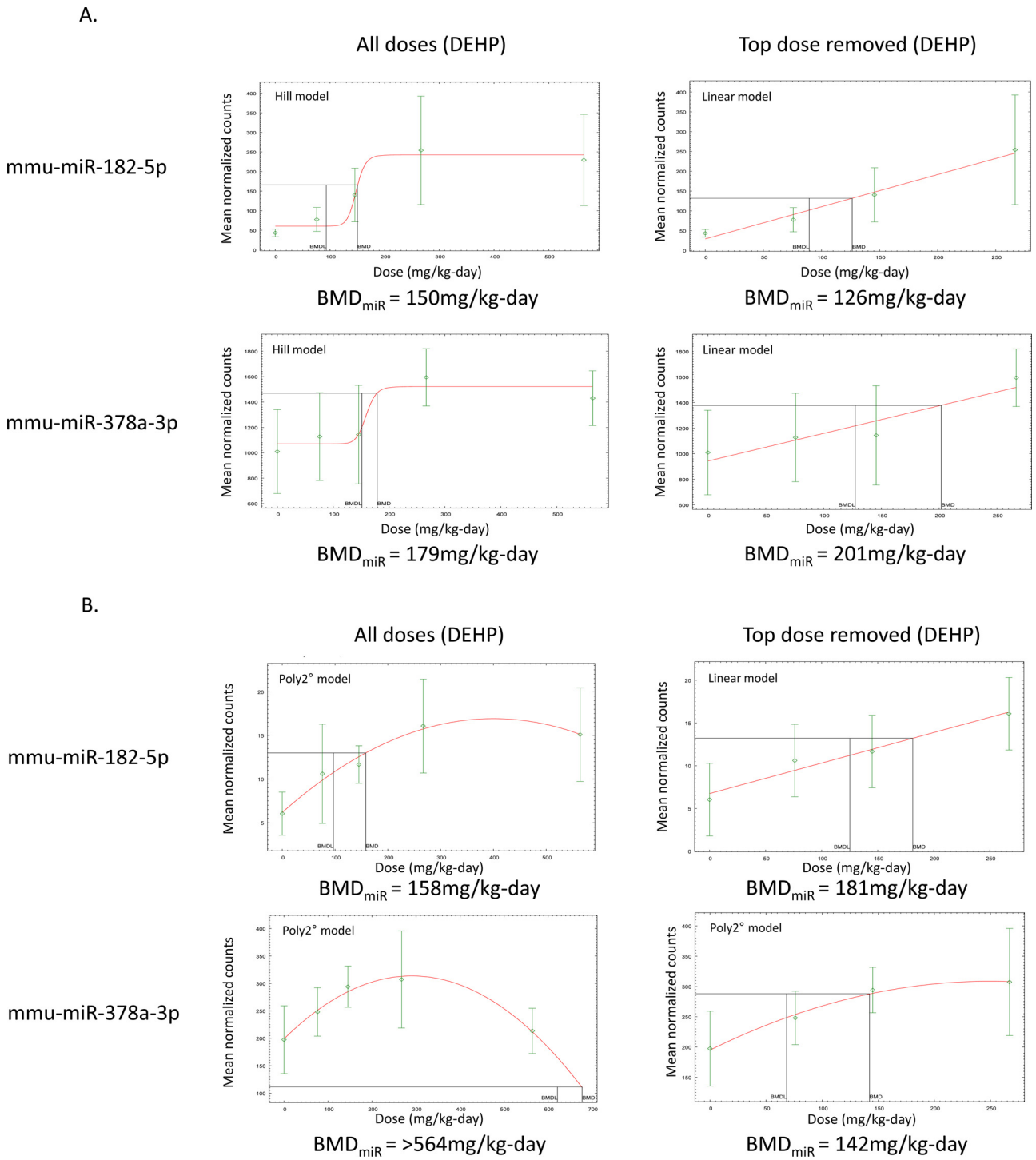


**Fig. 3. BMD analysis of mmu-miR-182-5p and mmu-miR-378a-3p using 7-day DEHP exposure data.** (**A**) Small RNA-seq data for the top two miRNA candidates were fit to the best response model, with and without top dose, using benchmark dose (BMD) analysis. (**B**) Modeling was repeated for the same miRNA candidates using ddPCR data, with and without top dose, using the best fit model. Doses were converted to mg dose per mouse weight (kg) each day. Both BMD and benchmark dose for lower confidence interval ($BMD_L$) are noted in each graph. See *Materials and Methods* for full procedure description.

mmu-let-7g − 5p was also analyzed. Using sequencing data, mmu-miR-20a-5p did not fit tested models (based on global goodness-of-fit > 0.1) and was not considered for further testing. For mmu-miRs-182 and -378a, response to the 6000 ppm dose of DEHP was similar to or lower than the response to the 3000 ppm dose; therefore, data for the highest dose were excluded to see if model fits improved analysis of the lower dose trend. AIC values (lower), local scaled residuals (nearer to 0), and overall visual fit improved; therefore, only 3 doses were used to calculate $BMD_{miR}$ values (Fig. 3A, right panel). Similar to the sequencing data, better low dose fit was achieved by dropping the high dose for mmu-miRs-182 − 5p and -378a − 3p using ddPCR data (Fig. 3B).

Referent estimates for $BMD_T$ (transcriptional) and $BMD_A$ (apical) endpoints [8,32,39] were compared to $BMD_{miR}$ values for all 3 phthalates (compare Fig. 4 with Supplemental Figs. 4 and 5). Of the miRNAs analyzed, mmu-miRs-182 − 5p and -378a − 3p best distinguished DEHP from BBP and DNOP. Rank potencies for mmu-miR-182 − 5p were

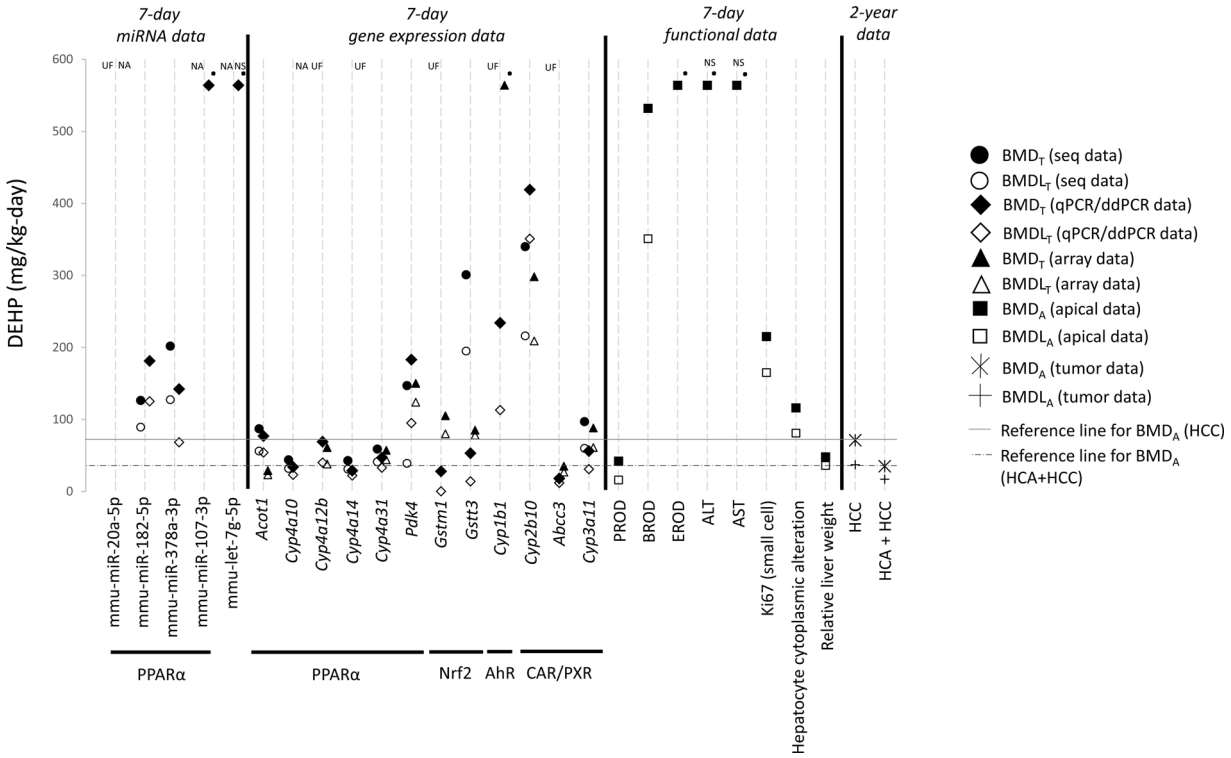


**Fig. 4. BMD analyses for miRNA, gene expression, apical, and 2-year tumor data based on DEHP exposure in mice.** Benchmark dose (BMD; closed shapes) and BMD lower confidence values (BMDL; open shapes) were calculated for select miRNA candidates and summarized for mRNA, apical measurements, and 2-year hepatocellular carcinoma (HCC) ± hepatocellular adenoma (HCA) based on previous calculations [8,32,39]. Where available, sequencing (circles), PCR (diamonds), and microarray (triangles) data were used to calculate transcriptomic ($_T$; here, both miRNA and mRNA) values. Associated pathways or transcriptional factors associated with these transcripts are marked below the gene/miRNA names. Functional apical ($_A$) BMD values, including measurements of CYP activity (PROD, BROD, EROD), liver enzymes (ALT and AST); small cell proliferation (Ki67), hepatocyte cytoplasmic alterations, and liver weight were derived from Lake et al. (2016) and denoted as squares. Exposure thresholds for HCC and HCC + HCA are based on two-year data, calculated in Wood et al. (2014), and shown for reference as asterisks/solid line (BMD) or pluses/broken lines (BMDL). Special notations for BMD values: ˙ = BMD greater than top dose tested; UF = the response was dose-related but was an Unacceptable Fit (global goodness of fit $p$-value < 0.1); NS = not significance compared to control values for any dose tested; NA = measurement not available.

DEHP > BBP > DNOP, while potencies for mmu-miR-378a-3p were DEHP > DNOP > BBP. Of note, $BMD_{miR}$ values were approximately twice $BMD_T$ values for expression of the most sensitive genes (*Acot1, Cyp4a12b,* and *Cyp4a14* for PPARα; *Gstm1* for *Nrf2*/oxidative stress; and *Abcc3* for CAR/PXR). $BMD_{miR}$ values were also well above $BMD_A$ values calculated for liver tumor incidence after 2 years of exposure but lower than many of the $BMD_A$ values for DEHP at 7 days, with the exception of hepatocyte cytoplasmic alteration (similar to $BMD_{miR}$ values) and relative liver weight (lower than $BMD_{miR}$ values).

### 3.4. Serum microRNA measurements

In addition to liver miRNA measurements, we also tested whether miRNA profiles in blood would reflect liver alterations due to DEHP exposure and potentially serve as a non-invasive measurement (and putative basis for POD determinations). MiRNAs were isolated from archived study serum samples, and mmu-miRs-182−5p and -378a−3p were measured at all 7-day DEHP doses at 7 days and the highest DEHP dose at 28 days using ddPCR (Fig. 5A and B). We observed no significant increase in miRNA levels at either timepoint, although both mmu-miRs-182−5p and -378a-3p trended upward after 28 days.

## 4. Discussion

The primary goals of this study were to identify early miRNA indicators of PPARα pathway perturbation and evaluate dose response characteristics. We observed modest but statistically significant responses in liver miRNA profiles after 7 days of treatment with the reference PPARα activator DEHP. Many of the miRNAs altered at 7 days were also observed after 28 days of treatment. Approximately one-third of the DEmiRs at 7 days were dose-responsive and many were linked to PPARα signaling according to pathway analysis and mouse knockout datasets. Benchmark dose estimates (or the calculated threshold doses for an adverse chemical effect) for mmu-miRs-182−5p and -378a−3p were lower for DEHP compared to the two other phthalates (BBP and DNOP) with less known PPARα activity [8]. We further tested if these miRNA candidates could be measured in the blood and reflect dose-responses observed in the liver. MiRs-182−5p and -378a−3p were detectable in blood using ddPCR and showed an increased trend but were not significantly different by 28 days at the highest exposure level of DEHP. Overall, the study indicates that miRNAs measured from a target organ or tissue of interest can display early dose-responsive patterns linked to the predominant signaling pathway.

We examined the early alterations of miRNA expression under the premise that measuring small noncoding RNA could reduce the complexity and variability of mRNA biomarkers. This idea is based on observations that a single miRNA can potentially have hundreds of gene targets, either through direct regulation or through a feed-forward regulatory loop with transcription factors [42]. As a consequence, dysregulation of a small number of select miRNAs may potentially impact an entire signaling pathway [43] and provide greater biological coverage than single gene biomarkers [44], which in many cases are arbitrarily selected. In our study, most of the dose-responsive miRNAs after 7 days of DEHP exposure were associated with the PPARα pathway, either through pathway analysis that indicated PPARα was an upstream mediator of miRNA expression or by association of previously

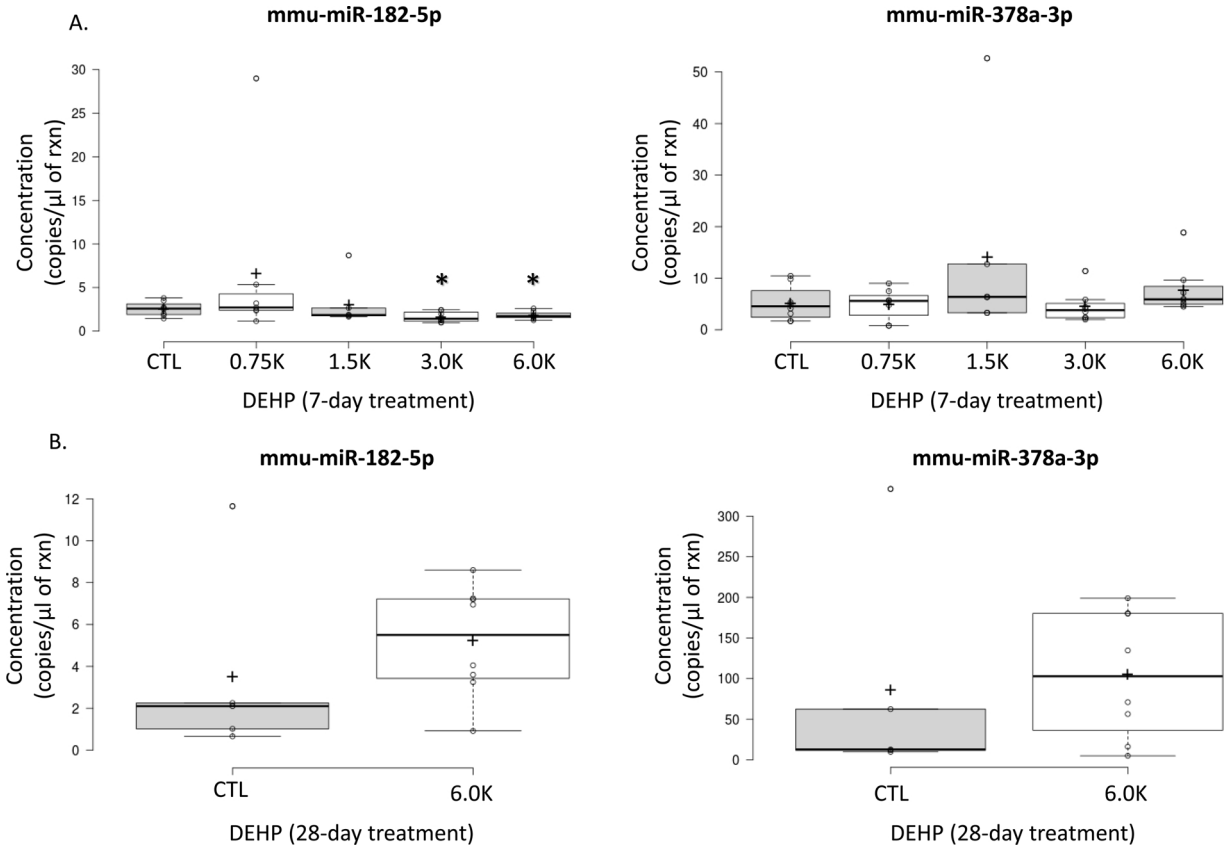


**Fig. 5. Serum measurements of mmu-miR-182-5p and mmu-miR-378a-3p.** Digital drop PCR (ddPCR) was performed to measure miRNA candidates in serum isolated from DEHP treated and control mice from (**A**) 7-day and (**B**) 28-day exposures. Box plots of data shown. * = significant based on Mann-Whitney *U* test (*p*-value < 0.05). n = 6-8.

generated data in PPARα-wild type and *null* mice exposed to a PPARα agonist [27]. This suggests that many of the 7-day, dose-responsive miRNAs are downstream of PPARα. This does not discount that the miRNAs may be part of a regulatory loop with PPARα or other mechanisms that may contribute to eventual liver tumor formation. Indeed multiple miRNAs that we observed altered by 28 days of DEHP exposure are known to target PPARα itself (e.g., miRs-10b, -141, -21a, -22, -21a, and -34a) [28]. Future studies should establish how these DEHP-responsive miRNAs are involved in up- or downstream regulation of PPARα and other transcriptional factors associated with an adverse outcome.

In our previous study [8], BMD analysis of early gene expression changes showed that $BMD_T$ estimates for select genes were more sensitive quantitative endpoints for stratifying chemicals based on MOA/AOP and predicting later-life effects compared to standard apical measures. However, there was also high variability noted for many of the dose-responsive genes. BMD estimates varied widely for many PPARα target genes, and gene expression data from global measurements pointed to multiple MOA/AOPs (e.g. CAR/PXR and oxidative stress,). DEHP induces liver cell toxicity at higher doses [32] and mediates a CAR/PXR response in addition to PPARα, which may have a minor contribution to the increase in liver tumor incidence observed in mice [37,38]. As with many transcriptional products, miRNAs are likely not exclusively regulated by a single transcription factor (which would reduce specificity as a biomarker). To further explore this idea in the DEHP data set, we can compare CAR/PXR-activated DEmiRs (determined by exposure to the CAR agonist, phenobarbital, in CAR/PXR-wild type and *null* mice) [26] to our PPARα-linked DEmiRs. Of the nine miRNAs that were CAR/PXR-dependent, four were also altered following 7- or 28-day exposure to DEHP (miRs-541−5p, -379−5p, -411−5p, and -541−5p). Importantly, all of these miRNAs were transcribed from the imprinted *Dio-Dlk3* chromosome 12 region, known to be responsive to CAR activation [45]. These miRNAs were *down-regulated* with DEHP (not upregulated as seen with PB exposure), indicating a suppression of the CAR/PXR-linked miRNAs. Previous work has also indicated that PPARα and CAR/PXR may play antagonist roles in gene expression regulation [38], further suggesting that down-regulation of these CAR/PXR-linked miRNAs may be suppressed by the predominant PPARα signal activation following DEHP exposure. This analysis supports the premise that altered miRNAs observed in our study is likely mediated by PPARα activity. However, caution is also warranted when attributing transcriptional responses to a single MOA.

Few studies other have measured miRNA liver response to PPARα agonists in rodents. In addition to the PPARα agonist, WY-14,643, exposure performed in PPARα-*null* and -*wild type* mice study previously referred to in our results [27], a comprehensive analysis of genotoxic and nongenotoxic chemical exposures in C57BL/6 J mice, liver miRNA alterations were measured in response to PPARα activators (DEHP, Wyeth-14,643, and diisodecyl phthalate) [46]. The overlapping DEmiRs of these three chemicals were surprisingly modest (seven total), however one of these miRNAs was miR-378a−3p, which we also identified as one of our two top DEHP-responsive candidates. Despite the different mouse strain used, we also observed 19 shared DEmiRs at either 7- or 28-day DEHP exposure with the Melis et al. study. One of these miRNAs, miR-155−5p, was also altered by the known PPARα agonist, clofibrate, in F344/DuCrl rats [9]. In this study, 20 miRNAs were measured on a PCR-based assay panel and the investigators observed lower expression of miR-122, -125a, -155, -199a−5p, and -199a−3p. Consistent with this finding, we also noted a significant reduction with 7 and/or 28 days of DEHP exposure in all of these candidates except miR-199a−5p. It was not clear from the study by Miousse et al. (2017) what other miRNAs were measured that were not

significantly altered with the exposures; therefore, it is unknown if our top-performing PPARα-linked candidates were also altered with clofibrate exposure in the model. Despite the limited miRNA data that has been generated in rodent liver in response to PPARα agonists, there are some indications of similar response with specific miRNAs. Future studies should focus on consistently responding miRNAs that are directly linked to activation of specific transcriptional factors in different model species.

To our knowledge, Miousse et al. [9] is the first report to derive BMD estimates from individual miRNA measurements. In their study, investigators evaluated a variety of epigenetic, metabolic, and apical endpoints following 7 days of exposure in male rats to the reference liver toxicants clofibrate and phenobarbital. The observed down-regulation of miRNAs was modest and not conducive to dose model fitting. In our study, we also observed a modest miRNA response and, not surprisingly, $BMD_{miR}$ estimates were higher than $BMD_T$ values of the most responsive PPARα target genes, as well as the $BMD_A$ estimates such as liver tumor incidence at 2 years. Based on this evidence, BMD estimates using short-term measurement of miRNAs do not suggest doses protective of apical outcomes, at least for the PPARα pathway. Similar to our findings, gene expression targets for nuclear receptors linked to known MOAs for each chemical provided the most conservative BMD estimates. Miousse et al. concluded that the combination of apical, transcriptional, epigenetic, and other early molecular-based changes increase the weight-of-evidence for a MOA and enhance prediction of toxicity following chemical exposures in the liver. A more recent study calculated BMD for various small RNAs (including miRNAs) in sperm as a measure of testicular toxicity in response to ethylene glycol monomethyl ether exposure in rats and compared it to the BMD of less sensitive phenotypic measurements of sperm count and health [47]. While the study focused on sequencing metrics (e.g., measuring read length) rather than identifying individual miRNA, the finding highlights further utility of quantifying small RNA as a unique measure of toxicity.

MiRNAs can be readily measured in blood and other accessible matrices, highlighting their potential value in biosurveillance programs. Exogenously expressed miRNAs are stable and resistant to degradation in biofluids because of their association with cell-derived exosomes, microvesicles, or other miRNA-associated components such as lipids and proteins [48,49]. There is also evidence that miRNAs can serve as mediators in a form of paracrine-like communication [50]. However, it is still unclear whether miRNAs released into biofluids can provide mechanistic information for a particular cellular or tissue response. In this study, we measured mmu-miRs-182−5p and -378a−3p levels in serum derived from mice treated for 7 and 28 days with DEHP to look for concordance with dose-responsive changes measured in the liver. Using ddPCR, we measured the presence of both miRNAs in the serum. There was an increasing trend at the highest exposure level of DEHP at 28 days but no significant group differences in serum miRNA concentrations after 7 or 28 days. Future studies of mmu-miRs-182−5p and -378a−3p in serum would likely require greater sample size and/or longer duration of exposure.

In a recent investigation into a human population with high levels of exposure to PFAS, the study authors found alterations of serum-based miRNA levels including miR-122−5p and PPARα-linked miRs-101−3p, -107, and 20a-5p [51]. MiR-122−5p is the most abundant miRNA in hepatocytes (~70 % of expressed miRNA) [52] and has been extensively studied as a liver toxicity biomarker [29]. However, it is unclear whether this miRNA in the serum indicates general leakage due to liver cell injury or secretion through exosomal or other cell-mediated release due to a specific mechanism. Although the data were not shown, we also included the measurement of liver-specific miR-122−5p in the current study in blood. Similar to traditional serum biomarkers of liver toxicity (alanine aminotransferase and sorbitol dehydrogenase) previously measured for this study [8], serum-derived miR-122−5p was not significantly different following 7 or 28 days of DEHP treatment compared to controls. This information, in combination with human PFAS data mentioned above, supports the idea that miR-122−5p is mediated predominantly via hepatocellular damage, with subsequent release into circulation. More broadly, this issue highlights the need to better understand the tissue-specificity of miRNA responses in the blood and their utility in screening for exposure to specific types of chemicals [29].

MiRNAs are small non-coding RNA molecules that may serve as biomarkers of chemical exposure and susceptibility to adverse health effects. In this study, we examined miRNAs as short-term indicators of PPARα pathway perturbation in the liver. Several miRNAs were identified and shown to be dose-responsive and the majority were linked to the known primary MOA/AOP for DEHP-mediated rodent liver tumor formation. However, given the limited dynamic range for miRNA responses, mRNA targets provided BMD values more aligned with apical estimates. Dose-responsive miRNAs were also detected in the blood but did not show significant treatment effects or concordance with liver miRNA changes. This information indicates miRNAs may be short-term indicators of target pathway disruptions of concern when determining chemical effects. Future work is needed to determine relevant applications in both nonclinical safety and epidemiologic studies.

## 5. Disclaimer

The research described in this article has been reviewed by the U.S. EPA and approved for publication. Approval does not signify that the contents necessarily reflect the views and the policies of the Agency. Mention of trade names or commercial products does not constitute endorsement or recommendation for use.

## Funding

Funding was provided by the U.S. EPA Office of Research and Development.

## Declaration of Competing Interest

The authors declare no conflict of interest.

## Acknowledgements

The authors would like to Drs. Chris Corton and Christopher Lau for technical review and constructive comments on this manuscript.

## Appendix A. Supplementary data

Supplementary material related to this article can be found, in the online version, at doi:https://doi.org/10.1016/j.toxrep.2020.06.006.

## References

[1] N.R. Council, Toxicity Testing in the 21st Century: A Vision and a Strategy, The National Academies Press, Washington, DC, 2007.
[2] D. Krewski, D. Acosta Jr., M. Andersen, H. Anderson, J.C. Bailar 3rd, K. Boekelheide, R. Brent, G. Charnley, V.G. Cheung, S. Green Jr.et al., Toxicity testing in the 21st century: a vision and a strategy, J. Toxicol. Environ. Health B Crit. Rev. 13 (2010) 51–138.
[3] G.T. Ankley, R.S. Bennett, R.J. Erickson, D.J. Hoff, M.W. Hornung, R.D. Johnson, D.R. Mount, J.W. Nichols, C.L. Russom, P.K. Schmieder, et al., Adverse outcome pathways: a conceptual framework to support ecotoxicology research and risk assessment, Environ. Toxicol. Chem. 29 (2010) 730–741.
[4] A.R. Boobis, S.M. Cohen, V. Dellarco, D. McGregor, M.E. Meek, C. Vickers, D. Willcocks, W. Farland, IPCS framework for analyzing the relevance of a cancer mode of action for humans, Crit. Rev. Toxicol. 36 (2006) 781–792.
[5] R. Thomas, R.S. Thomas, S.S. Auerbach, C.J. Portier, Biological networks for predicting chemical hepatocarcinogenicity using gene expression data from treated mice and relevance across human and rat species, PLoS One 8 (2013) e63308.
[6] R.S. Thomas, H.J. Clewell 3rd, B.C. Allen, L. Yang, E. Healy, M.E. Andersen, Integrating pathway-based transcriptomic data into quantitative chemical risk assessment: a five chemical case study, Mutat. Res. 746 (2012) 135–143.

[7] R.S. Thomas, S.C. Wesselkamper, N.C. Wang, Q.J. Zhao, D.D. Petersen, J.C. Lambert, I. Cote, L. Yang, E. Healy, M.B. Black, et al., Temporal concordance between apical and transcriptional points of departure for chemical risk assessment, Toxicol. Sci. 134 (2013) 180–194.
[8] A.D. Lake, C.E. Wood, V.S. Bhat, B.N. Chorley, G.K. Carswell, Y.M. Sey, E.M. Kenyon, B. Padnos, T.M. Moore, A.H. Tennant, et al., Dose and effect thresholds for early key events in a PPARalpha-Mediated mode of action, Toxicol. Sci. 149 (2016) 312–325.
[9] I.R. Miousse, L.A. Murphy, H. Lin, M.R. Schisler, J. Sun, M.G. Chalbot, R. Sura, K. Johnson, M.J. LeBaron, I.G. Kavouras, et al., Dose-response analysis of epigenetic, metabolic, and apical endpoints after short-term exposure to experimental hepatotoxicants, Food Chem. Toxicol. (2017).
[10] J.E. Rager, S.S. Auerbach, G.A. Chappell, E. Martin, C.M. Thompson, R.C. Fry, Benchmark dose modeling estimates of the concentrations of inorganic arsenic that induce changes to the neonatal transcriptome, proteome, and epigenome in a pregnancy cohort, Chem. Res. Toxicol. 30 (2017) 1911–1920.
[11] H. Dong, S. Gill, I.H. Curran, A. Williams, B. Kuo, M.G. Wade, C.L. Yauk, Toxicogenomic assessment of liver responses following subchronic exposure to furan in Fischer F344 rats, Arch. Toxicol. 90 (2016) 1351–1367.
[12] R.S. Thomas, T.M. O'Connell, L. Pluta, R.D. Wolfinger, L. Yang, T.J. Page, A comparison of transcriptomic and metabonomic technologies for identifying biomarkers predictive of two-year rodent cancer bioassays, Toxicol. Sci. 96 (2007) 40–46.
[13] N. Ryan, B. Chorley, R.R. Tice, R. Judson, J.C. Corton, Moving Toward Integrating Gene Expression Profiling Into High-Throughput Testing: A Gene Expression Biomarker Accurately Predicts Estrogen Receptor alpha Modulation in a Microarray Compendium, Toxicol. Sci. 151 (2016) 88–103.
[14] J. Rooney, K. Oshida, N. Vasani, B. Vallanat, N. Ryan, B.N. Chorley, X. Wang, D.A. Bell, K.C. Wu, L.M. Aleksunes, et al., Activation of Nrf2 in the liver is associated with stress resistance mediated by suppression of the growth hormone-regulated STAT5b transcription factor, PLoS One 13 (2018) e0200004.
[15] J. Rooney, T. Hill 3rd, C. Qin, F.D. Sistare, J.C. Corton, Adverse outcome pathway-driven identification of rat liver tumorigens in short-term assays, Toxicol. Appl. Pharmacol. 356 (2018) 99–113.
[16] H.H. Li, R. Chen, D.R. Hyduke, A. Williams, R. Frotschl, H. Ellinger-Ziegelbauer, R. O'Lone, C.L. Yauk, J. Aubrecht, A.J. Fornace Jr., Development and validation of a high-throughput transcriptomic biomarker to address 21st century genetic toxicology needs, Proc Natl Acad Sci U S A 114 (2017) E10881–E10889.
[17] D. Mav, R.R. Shah, B.E. Howard, S.S. Auerbach, P.R. Bushel, J.B. Collins, D.L. Gerhold, R.S. Judson, A.L. Karmaus, E.A. Maull, et al., A hybrid gene selection approach to create the S1500+ targeted gene sets for use in high-throughput transcriptomics, PLoS One 13 (2018) e0191105.
[18] S. Jonas, E. Izaurralde, Towards a molecular understanding of microRNA-mediated gene silencing, Nat. Rev. Genet. 16 (2015) 421–433.
[19] S. Gu, M.A. Kay, How do miRNAs mediate translational repression? Silence 1 (2010) 11.
[20] E. Woolard, B.N. Chorley, The role of noncoding RNAs in Gene regulation, Chapter 3-1, in: S.D. McCullough, D.C. Dolinoy (Eds.), Toxicoepigenetics, Academic Press, 2019, pp. 217–235.
[21] J. Lu, A.G. Clark, Impact of microRNA regulation on variation in human gene expression, Genome Res. 22 (2012) 1243–1254.
[22] P.M. Clark, P. Loher, K. Quann, J. Brody, E.R. Londin, I. Rigoutsos, Argonaute CLIP-Seq reveals miRNA targetome diversity across tissue types, Sci. Rep. 4 (2014) 5947.
[23] X. Li, J.J. Cassidy, C.A. Reinke, S. Fischboeck, R.W. Carthew, A microRNA imparts robustness against environmental fluctuation during development, Cell 137 (2009) 273–282.
[24] R. Blevins, L. Bruno, T. Carroll, J. Elliott, A. Marcais, C. Loh, A. Hertweck, A. Krek, N. Rajewsky, C.Z. Chen, et al., microRNAs regulate cell-to-cell variability of endogenous target gene expression in developing mouse thymocytes, PLoS Genet. 11 (2015) e1005020.
[25] J. Lu, G. Getz, E.A. Miska, E. Alvarez-Saavedra, J. Lamb, D. Peck, A. Sweet-Cordero, B.L. Ebert, R.H. Mak, A.A. Ferrando, et al., MicroRNA expression profiles classify human cancers, Nature 435 (2005) 834–838.
[26] R. Luisier, H. Lempiainen, N. Scherbichler, A. Braeuning, M. Geissler, V. Dubost, A. Muller, N. Scheer, S.D. Chibout, H. Hara, et al., Phenobarbital induces cell cycle transcriptional responses in mouse liver humanized for constitutive androstane and pregnane x receptors, Toxicol. Sci. 139 (2014) 501–511.
[27] Y.M. Shah, K. Morimura, Q. Yang, T. Tanabe, M. Takagi, F.J. Gonzalez, Peroxisome proliferator-activated receptor alpha regulates a microRNA-mediated signaling cascade responsible for hepatocellular proliferation, Mol. Cell. Biol. 27 (2007) 4238–4247.
[28] D. Portius, C. Sobolewski, M. Foti, MicroRNAs-dependent regulation of PPARs in metabolic diseases and cancers, PPAR Res. 2017 (2017) 7058424.
[29] A.H. Harrill, S.D. McCullough, C.E. Wood, J.J. Kahle, B.N. Chorley, MicroRNA biomarkers of toxicity in biological matrices, Toxicol. Sci. 152 (2016) 264–272.
[30] J.C. Corton, M.L. Cunningham, B.T. Hummer, C. Lau, B. Meek, J.M. Peters, J.A. Popp, L. Rhomberg, J. Seed, J.E. Klaunig, Mode of action framework analysis for receptor-mediated toxicity: The peroxisome proliferator-activated receptor alpha (PPARalpha) as a case study, Crit. Rev. Toxicol. 44 (2014) 1–49.
[31] J.E. Klaunig, M.A. Babich, K.P. Baetcke, J.C. Cook, J.C. Corton, R.M. David, J.G. DeLuca, D.Y. Lai, R.H. McKee, J.M. Peters, et al., PPARalpha agonist-induced rodent tumors: modes of action and human relevance, Crit. Rev. Toxicol. 33 (2003) 655–780.
[32] C.E. Wood, M.P. Jokinen, C.L. Johnson, G.R. Olson, S. Hester, M. George, B.N. Chorley, G. Carswell, J.H. Carter, C.R. Wood, et al., Comparative time course profiles of phthalate stereoisomers in mice, Toxicol. Sci. 139 (2014) 21–34.
[33] B.D. Abbott, Review of the expression of peroxisome proliferator-activated receptors alpha (PPAR alpha), beta (PPAR beta), and gamma (PPAR gamma) in rodent and human development, Reprod. Toxicol. 27 (2009) 246–257.
[34] J.C. DeWitt, A. Shnyra, M.Z. Badr, S.E. Loveless, D. Hoban, S.R. Frame, R. Cunard, S.E. Anderson, B.J. Meade, M.M. Peden-Adams, et al., Immunotoxicity of perfluorooctanoic acid and perfluorooctane sulfonate and the role of peroxisome proliferator-activated receptor alpha, Crit. Rev. Toxicol. 39 (2009) 76–94.
[35] B. Thoolen, R.R. Maronpot, T. Harada, A. Nyska, C. Rousseaux, T. Nolte, D.E. Malarkey, W. Kaufmann, K. Kuttler, U. Deschl, et al., Proliferative and nonproliferative lesions of the rat and mouse hepatobiliary system, Toxicol. Pathol. 38 (2010) 5S-81S..
[36] J.D. Tugwood, I. Issemann, R.G. Anderson, K.R. Bundell, W.L. McPheat, S. Green, The mouse peroxisome proliferator activated receptor recognizes a response element in the 5' flanking sequence of the rat acyl CoA oxidase gene, EMBO J. 11 (1992) 433–439.
[37] Y. Ito, O. Yamanoshita, N. Asaeda, Y. Tagawa, C.H. Lee, T. Aoyama, G. Ichihara, K. Furuhashi, M. Kamijima, F.J. Gonzalez, et al., Di(2-ethylhexyl)phthalate induces hepatic tumorigenesis through a peroxisome proliferator-activated receptor alpha-independent pathway, J. Occup. Health 49 (2007) 172–182.
[38] H. Ren, L.M. Aleksunes, C. Wood, B. Vallanat, M.H. George, C.D. Klaassen, J.C. Corton, Characterization of peroxisome proliferator-activated receptor alpha–independent effects of PPARalpha activators in the rodent liver: di-(2-ethylhexyl) phthalate also activates the constitutive-activated receptor, Toxicol. Sci. 113 (2010) 45–59.
[39] S.D. Hester, V. Bhat, B.N. Chorley, G. Carswell, W. Jones, L.C. Wehmas, C.E. Wood, Editor's Highlight: Dose-Response Analysis of RNA-Seq Profiles in Archival Formalin-Fixed Paraffin-Embedded Samples, Toxicol. Sci. 154 (2016) 202–213.
[40] EPA, Benchmark Dose Technical Guidance, EPA Risk Assessment Forum EPA/100/R-12/001, 2012.
[41] R.S. Thomas, B.C. Allen, A. Nong, L. Yang, E. Bermudez, H.J. Clewell 3rd, M.E. Andersen, A method to integrate benchmark dose estimates with genomic data to assess the functional effects of chemical exposure, Toxicol. Sci. 98 (2007) 240–248.
[42] R. Shalgi, D. Lieber, M. Oren, Y. Pilpel, Global and local architecture of the mammalian microRNA-transcription factor regulatory network, PLoS Comput. Biol. 3 (2007) e131.
[43] C.D. Johnson, A. Esquela-Kerscher, G. Stefani, M. Byrom, K. Kelnar, D. Ovcharenko, M. Wilson, X. Wang, J. Shelton, J. Shingara, et al., The let-7 microRNA represses cell proliferation pathways in human cells, Cancer Res. 67 (2007) 7713–7722.
[44] S. Freiesleben, M. Hecker, U.K. Zettl, G. Fuellen, L. Taher, Analysis of microRNA and gene expression profiles in multiple sclerosis: integrating interaction data to uncover regulatory mechanisms, Sci. Rep. 6 (2016) 34512.
[45] H. Lempiainen, A. Muller, S. Brasa, S.S. Teo, T.C. Roloff, L. Morawiec, N. Zamurovic, A. Vicart, E. Funhoff, P. Couttet, et al., Phenobarbital mediates an epigenetic switch at the constitutive androstane receptor (CAR) target gene Cyp2b10 in the liver of B6C3F1 mice, PLoS One 6 (2011) e18216.
[46] J.P. Melis, K.W. Derks, T.E. Pronk, P. Wackers, M.M. Schaap, E. Zwart, W.F. van Ijcken, M.J. Jonker, T.M. Breit, J. Pothof, et al., In vivo murine hepatic microRNA and mRNA expression signatures predicting the (non-)genotoxic carcinogenic potential of chemicals, Arch. Toxicol. 88 (2014) 1023–1034.
[47] A.R. Stermer, G. Reyes, S.J. Hall, K. Boekelheide, Small RNAs in rat sperm are a predictive and sensitive biomarker of exposure to the testicular toxicant ethylene glycol monomethyl ether, Toxicol. Sci. 169 (2019) 399–408.
[48] X. Chen, H. Liang, J. Zhang, K. Zen, C.Y. Zhang, Secreted microRNAs: a new form of intercellular communication, Trends Cell Biol. 22 (2012) 125–132.
[49] A. Etheridge, I. Lee, L. Hood, D. Galas, K. Wang, Extracellular microRNA: a new source of biomarkers, Mutat. Res. 717 (2011) 85–90.
[50] Y. Zhang, D. Liu, X. Chen, J. Li, L. Li, Z. Bian, F. Sun, J. Lu, Y. Yin, X. Cai, et al., Secreted monocytic miR-150 enhances targeted endothelial cell migration, Mol. Cell 39 (2010) 133–144.
[51] Y. Xu, S. Jurkovic-Mlakar, Y. Li, K. Wahlberg, K. Scott, D. Pineda, C.H. Lindh, K. Jakobsson, K. Engstrom, Association between serum concentrations of perfluoroalkyl substances (PFAS) and expression of serum microRNAs in a cohort highly exposed to PFAS from drinking water, Environ. Int. 136 (2020) 105446.
[52] J. Chang, E. Nicolas, D. Marks, C. Sander, A. Lerro, M.A. Buendia, C. Xu, W.S. Mason, T. Moloshok, R. Bort, et al., miR-122, a mammalian liver-specific microRNA, is processed from hcr mRNA and may downregulate the high affinity cationic amino acid transporter CAT-1, RNA Biol. 1 (2004) 106–113.